Calcipotriol Attenuates Form Deprivation Myopia Through a Signaling Pathway Parallel to TGF-β2–Induced Increases in Collagen Expression

Shiming Jiao,[1,2] Peter Sol Reinach,[1,2] Chengjie Huang,[1,2] Lan Yu,[1,2] Huiman Zhuang,[1,2] Hongli Ran,[1,2] Fei Zhao,[1–5] Nethrajeith Srinivasalu,[1,2] Jia Qu,[1,2,4,5] and Xiangtian Zhou[1–5]

[1]School of Optometry and Ophthalmology and Eye Hospital, Wenzhou Medical University, Wenzhou, Zhejiang, China
[2]State Key Laboratory of Ophthalmology, Optometry and Visual Science, Eye Hospital, Wenzhou Medical University, Wenzhou, Zhejiang, China
[3]Research Unit of Myopia Basic Research and Clinical Prevention and Control, Chinese Academy of Medical Sciences, Wenzhou, Zhejiang, China
[4]Oujiang Laboratory, Zhejiang Lab for Regenerative Medicine, Vision and Brain Health, Wenzhou, Zhejiang, China
[5]National Clinical Research Center for Ocular Diseases, Wenzhou, Zhejiang, China

Correspondence: Xiangtian Zhou and Jia Qu, School of Ophthalmology and Optometry and Eye Hospital, Wenzhou Medical University, 270 Xueyuan Road, Wenzhou, Zhejiang 325027, China; zxt@mail.eye.ac.cn, jqu@wmu.edu.cn.

SJ and PSR contributed equally to this work.

Received: June 18, 2022
Accepted: December 27, 2022
Published: February 1, 2023

Citation: Jiao S, Reinach PS, Huang C, et al. Calcipotriol attenuates form deprivation myopia through a signaling pathway parallel to TGF-β2–induced increases in collagen expression. *Invest Ophthalmol Vis Sci.* 2023;64(2):2. https://doi.org/10.1167/iovs.64.2.2

Purpose. To determine the role of calcipotriol, a vitamin D3 analogue, in myopia development and altering the expression of scleral α1 chain of type I collagen (*Col1*α*1*) in mice. We also aimed to identify if the signaling pathway mediating the above changes is different from the one involved in transforming growth factor β2 (TGF-β2)–mediated increases of COL1A1 in cultured human scleral fibroblasts (HSFs).

Methods. C57BL/6J mice were either intraperitoneally injected with calcipotriol and subjected to form deprivation (FD) or exposed to normal refractive development for 4 weeks. Scleral vitamin D receptor (*Vdr*) expression was knocked down using a Sub-Tenon's capsule injection of an adeno-associated virus–packaged short hairpin RNA (AAV8-shRNA). Refraction and biometric measurements evaluated myopia development. A combination of knockdown and induction strategies determined the relative contributions of the vitamin D3 and the TGF-β2 signaling pathways in modulating COL1A1 expression in HSFs.

Results. Calcipotriol injections suppressed FD-induced myopia (FDM), but it had no significant effect on normal refractive development. AAV8-shRNA injection reduced *Vdr* mRNA expression by 42% and shifted the refraction toward myopia (-3.15 ± 0.99D, means $\pm$ SEM) in normal eyes. In HSFs, VDR knockdown reduced calcipotriol-induced rises in COL1A1 expression, but it did not alter TGF-β2–induced increases in COL1A1 expression. Additionally, TGF-β2 augmented calcipotriol-induced rises in COL1A1 expression. TGF-β receptor (TGFBRI/II) knockdown blunted TGF-β2–induced increases in COL1A1 expression, whereas calcipotriol-induced increases in VDR and COL1A1 expression levels were unaltered.

Conclusions. Scleral vitamin D3 inhibits myopia development in mice, potentially by activating a VDR-dependent signaling pathway and increasing scleral COL1A1 expression levels.

Keywords: vitamin D3, TGF-β2, collagen, sclera, myopia

Myopia is a major sight-compromising condition, which increasingly detracts from the quality of life and causes numerous socioeconomic problems worldwide.[1,2] Of particular concern is its alarmingly high incidence of 85% to 95% among young individuals of East Asian origin.[3,4] This condition results from scleral thinning due to extracellular matrix (ECM) remodeling and decreases in the accumulation of collagen (especially the type I collagen, COL1A1).[5,6] This reduction is due to declines in its synthesis and increases in its degradation. These responses accompany maladaptive increases in optical axis elongation whose etiology is not yet fully understood. Genetic and environmental factors contribute to myopia, as evidenced by studies on genetic associations and outdoor activities, respectively impacting this condition.[7–10]

There is controversial evidence that an inverse relationship exists between serum vitamin D3 levels and myopia severity since lower blood vitamin D3 concentrations are associated with an increased risk of myopia.[11–15] Another indication of this association is based on possible functional and positional involvement of its receptor, vitamin D receptor (*VDR*), in myopia. It is located on chromosome 12, near the region of q21.2–24.12 (36.59 cM, MYP3 locus). A whole-genome linkage scan suggested significant modulation of myopia.[10,16] However, other studies showed irrespective of the time spent outdoors that variations in

serum vitamin D3 levels were unrelated to the risks of myopia development.[17–19] It must be noted that vitamin D3 content in these studies was measured in blood serum and a cause–effect relationship between vitamin D3 levels and ocular biometry could not be established. Therefore, experimental animal models and in vitro experiments are still needed to confirm that vitamin D3 supplementation and activation of its receptor-linked signaling inhibit myopia progression.

Vitamin D3 is supplied by both dietary consumption and ambient UVB light exposure that together induce its synthesis in the skin. Calcipotriol is a synthetic vitamin D3 analogue with a high binding affinity for VDR.[20,21] Such an interaction has tissue-specific effects on COL1A1 expression levels, a major scleral ECM component. In other multiple organs, low levels of vitamin D3 are instead associated with increases in fibrosis in different pathologic conditions.[22–24] On the other hand, transforming growth factor $\beta 2$ (TGF-$\beta 2$) promotes the synthesis of COL1A1 in scleral fibroblasts.[25] Declines in TGF-β expression levels are likely associated with decreases in scleral collagen content during myopia development.[25,26] Furthermore, activation of the vitamin D3 signaling pathway can attenuate TGF-β–induced fibrosis in different tissues and organs.[27–30] It is relevant to determine if vitamin D3–linked signaling interacts with the TGF-β–linked pathway to modulate COL1A1 expression and subsequently suppresses myopia development. Such insight may clarify the identity of alternative targets for improved therapeutic management of scleral ECM remodeling during myopia progression.

We show here that calcipotriol suppresses form deprivation (FD)–induced declines in *Col1α1* expression and inhibits myopia progression through a *Vdr*-dependent signaling pathway in mice. TGF-$\beta 2$–induced increases in COL1A1 expression are instead mediated through a VDR-independent signaling pathway in cultured human scleral fibroblasts (HSFs).

Materials and Methods

Animal Experiments

The treatment and care of the animals were conducted according to the ARVO statement for the use of animals in ophthalmic and vision research. The protocol for handling animals was approved by the Animal Care and Ethics Committee at Wenzhou Medical University, Wenzhou, China. Animals were raised in standard mice cages at the animal facility of this institution. The temperature was maintained at 22 ± 2°C under a 12-hour light/dark cycle, with food and water available ad libitum.

Form Deprivation and Ocular Measurements

Monocular FD-induced myopia (FDM) was induced by occluding one randomly chosen eye with a translucent diffuser in the 3-week-old male C57BL/6J mice, which were divided into two groups as previously described.[31] In one group, their eyes were form deprived (labeled as FD-T) for either 2 ($n = 7$) or 4 weeks ($n = 30$), and the untreated eye constituted the fellow eye control group (designated FD-F). Mice in the other group were untreated and served as age-matched normal controls (designated NC; $n = 5$ and 46, at 2 and 4 weeks, respectively). Before and after the FD periods, refraction was measured using an eccentric infrared photorefractor. The vitreous chamber depth (VCD, from the posterior lens surface to the vitreous–retina interface) and axial length (AL, from the anterior corneal surface to the vitreous–retina interface) were measured using a custom-made spectral-domain optical coherence tomography system. After ocular measurements, the mice were injected intraperitoneally with a mixture of ketamine (96 mg/kg) and xylazine (14.4 mg/kg) and euthanized. The eyes were enucleated to isolate the sclera as described previously.[31] Briefly, the eyeball was snipped off the extraocular muscles and placed in a 35-mm petri dish on ice. The cornea and lens were carefully removed, leaving an eye cup behind on which the vitreous was squeezed out. The retina and choroid were then scrapped off to obtain a clean sclera. All surgical instruments were cleaned with RNaseZap RNase Decontamination Solution (AM9782; Invitrogen, Carlsbad, CA, USA) to avoid RNA degradation. The sclera was then immediately immersed in RNA*later* (Ambion, Foster City, CA, USA) in a microfuge tube and stored at 4°C overnight. The RNA*later* was removed the next day and the sclera was stored at −80°C until performing RNA extraction.

Construction of Adeno-Associated Virus Serotype 8–Short Hairpin RNA Expression Vector

At OBiO Technology (Shanghai, China), the cDNA sequence (1269 bp) of mouse *Vdr* (NM_009504.4) was constructed. Screening of shRNA sequences targeting mouse *Vdr* gene was performed in NIH-3T3 fibroblasts (ATCC, Manassas, VA, USA). The *Vdr* short hairpin RNA (shRNA) targeting sequences were 5′-GCTTCCACTTCAACGCTAT-3′. The *Vdr* shRNA and the scrambled control shRNA sequences were, respectively, ligated into the adeno-associated virus serotype 8 (AAV8)–shRNA shuttle vector to construct AAV8-shRNA-*Vdr* and AAV8-shRNA-scramble for AAV8 packaging. The titrated virus yields ranged from 10^{12} to 10^{13} genomic copies/mL.

Three-week-old wild-type mice ($n = 58$) were randomly separated into three different groups: 22 mice were transfected with *Vdr* shRNA, another 18 mice were injected with scrambled shRNA, and 18 noninjected mice served as the control (labeled as *Vdr* shRNA, scrambled shRNA, and NC, respectively). Ocular measurements were recorded before AAV8 injection (baseline) and 1, 2, 3, and 4 weeks later.

Cell Culture

Primary HSFs were established,[32] and the cells were seeded in T75 flasks in Dulbecco modified Eagle medium (12430; Gibco, Waltham, MA, USA), supplemented with 10% fetal bovine serum (10099141c; Gibco), 1% penicillin-streptomycin (15140-122; Gibco), and 2 mM GIBCO GlutaMAX (35050061; Gibco) until confluent. All cells were grown at 37°C under 5% CO_2 in a humidified incubator (Thermo Fisher, Waltham, MA, USA). They were passaged using 0.25% trypsin (25200072; Gibco) and transferred onto 35-mm culture dishes (Falcon; Becton, Dickinson and Company, Franklin Lake, NJ, USA) for drug treatments. All subsequent experiments were restricted to passages 6 to 9 in this study.

Drug Treatments

Calcipotriol (R&D; Minneapolis, MN, USA) was dissolved in dimethyl sulfoxide (DMSO; Sigma-Aldrich, St. Louis, MO, USA) at a concentration of 10 mM. TGF-$\beta 2$ (R&D) was dissolved in sterile 4 mM HCl (Jiutai, Wenzhou, China) containing 0.1% bovine serum albumin (Gibco) at a concen-

Investigative Ophthalmology & Visual Science

Table 1. Real-Time PCR Primer Base Sequences

Target	Species	Forward Primer (5′-3′)	Reverse Primer (5′-3′)	Length (bp)
Col1α1	Mouse	GAGAGCGAGGCCTTCCCGGA	GGGAGCCAGCGGGACCTTGT	131
Vdr	Mouse	GAATGTGCCTCGGATCTGTGG	ATGCGGCAATCTCCATTGAAG	150
Cyp24a1	Mouse	CATCGACCACCGCCTAGAGA	ACAGCAGCGTACAGTTCTTTC	104
Cyp27b1	Mouse	TGCTTGCGGATTGCTAACG	CCTTAGTCGTCGCACAAGGTC	144
18s	Mouse	CGGACACGGACAGGATTGAC	TGCCAGAGTCTCGTTCGTTATC	123
VDR	Human	GTGGACATCGGCATGATGAAG	GGTCGTAGGTCTTATGGTGGG	181
ACTB	Human	CCATGTACGTTGCTATCCAGGC	CTCCTTAATGTCACGCACGATTTCC	250
COL1A1	Human	CGAGCGTGGTGTGCAAGGTC	CTGCACCACGTTCACCAGGC	157

tration of 5 µg/mL. All stock reagents were aliquoted into smaller volumes and stored at −20°C for later use. The mice in different groups received daily intraperitoneal injections of the respective drugs without anesthesia using a microliter syringe attached to a 29-gauge needle. The visually unobstructed control mice received either DMSO ($n = 11$) or 0.1 mg/kg calcipotriol (Cal; $n = 10$) or 0.5 mg/kg Cal ($n = 11$) in their respective experimental groups. Likewise, the FD mice also received either DMSO ($n = 15$) or 0.1 mg/kg Cal ($n = 15$) or 0.5 mg/kg Cal ($n = 15$) in their experimental groups. Calcipotriol doses (i.e., 0.1 mg/kg or 0.5 mg/kg body weight) were injected after dissolving them in DMSO.

RNA Interference

Transforming growth factor β receptor 1 (*TGFBRI*) and transforming growth factor β receptor 2 (*TGFBRII*) are key receptors of the TGF-β signaling pathway, which are critical in scleral ECM remodeling. Small interfering RNA (siRNA) transfection was used to abrogate their gene function in HSFs. The HSFs were exposed to *VDR/TGFBRI/TGFBRII* siRNA and lipofectamine RNAiMAX (Invitrogen) according to the manufacturer's protocol. The siRNA oligonucleotides directed against the *VDR/TGFBRI/TGFBRII* mRNA or scrambled sequences were used as negative controls. The siRNAs were designed and synthesized by the Shanghai Gene Pharma Corporation (Shanghai, China). Their sequences are as follows:

"*VDR* siRNA": 5′-CCUGCUCAGAUCACUGUAUTT-3′
"*TGFBRI* siRNA": 5′-GGCTTAGTATTCTGGGAAA-3′
"*TGFBRII* siRNA": 5′-GAAGACGGCTCCCTAAACA-3′

and control with scrambled sequence: 5′-UUCUCCGAACG UGUCACGUTT-3′. Protein and gene expression analyses were carried out after 24 hours of transfection.

RNA Extraction and Quantitative RT-PCR

Two sclerae were pooled to form a single sample that was homogenized using a ball mill (MM400; Retsch, Dusseldorf, Germany). Total RNA was extracted using the RNeasy Fibrous Tissue Mini Kit (Qiagen, GmbH, Hilden, Germany) at room temperature according to the manufacturer's instructions. RNA from HSFs was extracted using TRIZOL reagent (Invitrogen). RNA concentration and purity were determined with a NanoDrop 2000 spectrophotometer (Thermo Fisher). On average, 800 ng and 400 ng RNA were obtained from the HSFs and mice scleral samples, respectively. They had a 260/280-nm optical density ratio of at least 1.9. cDNAs were synthesized in a 20-µL reaction using the M-MLV Reverse Transcriptase (Promega, Madison, WI, USA). Gene expression analysis was then carried out in duplicates with a SYBR green master mix (Applied Biosystems, Foster City, CA, USA) in a PCR system (ABI ViiA7 Real-Time PCR System; Applied Biosystems). PCR primer designs were obtained from the published data at the PrimerBank website (Table 1). The *Cyp24a1* (cytochrome P450 family 24 subfamily A member 1) and *Cyp27b1* (cytochrome P450 family 27 subfamily B member 1) genes modulate the activity of vitamin D3 through either inhibiting or increasing its activation, respectively.[33] Relative mRNA expression levels of each gene were normalized to the Ct value of the housekeeping gene, *ACTB* or *18S rRNA*, within each sample, and the fold change estimates were calculated using the $2^{-\Delta\Delta Ct}$ method.[34]

Western Blot Analysis

HSFs were harvested and lysed in a buffer containing Radio-Immunoprecipitation Assay (RIPA) buffer (Beyotime Biotechnology, Shanghai, China), phenylmethylsulfonyl fluoride (PMSF; Beyotime Biotechnology), and a protease inhibitor cocktail (EDTA-free Complete Mini; Roche, Basel, Switzerland), using a horizontal shaker (BG-orbitaIH; BayGene, Beijing, China) for 20 minutes at 4°C. The lysate was centrifuged at 13,000 × *g* for 10 minutes at 4°C, and the supernatant was removed to estimate the protein concentration using a BCA protein assay (Beyotime Biotechnology). The protein samples were stored at −80°C for later use. Electrophoretic separation of 50 µg protein samples was performed on a BG-subMINI horizontal electrophoresis apparatus (BayGene). Their content was resolved using 10% SDS-PAGE and blotted onto a nitrocellulose membrane (Millipore, Billerica, MA, USA). The membranes were washed in TBS (pH 7.4; Sangon Biotech, Shanghai, China), containing 0.1% Tween-20 (TBST), blocked with 5% (w/v) dry nonfat milk (Sangon Biotech) in TBST for 1 hour. They were then washed with TBST and incubated with primary antibodies for 16 hours at 4°C. After multiple rinsing, the membranes were incubated with secondary antibodies at room temperature for 2 hours. The membranes were then washed again and visualized with a SuperSignal West Femto Maximum Sensitivity Substrate (Thermo Fisher). Densitometric analysis was carried out using Adobe Photoshop CC 2015 (San Jose, CA, USA). Table 2 describes the antibodies used in Western blot analysis.

Table 2. Antibodies Used for Western Blot

Primary Antibodies	Corporation	Item Number	Dilution
Collagen I	Abcam	ab88147	1:2000
α-Tubulin	Abcam	ab7291	1:2000
VDR	Abcam	ab3508	1:1000
Secondary antibodies			
Goat anti-mouse IgG (H+L)	Invitrogen	31431	1:10,000
Goat anti-rabbit IgG (H+L)	Invitrogen	31466	1:10,000

Investigative Ophthalmology & Visual Science

Image Analysis of Confocal Microscopy Immunofluorescence

HSFs were fixed in freshly prepared 4% paraformaldehyde for 30 minutes at 4°C and washed three times in PBS for 5 minutes with a 0.1 M PBS blocking solution containing 6% normal donkey serum, 1% bovine serum albumin, and 0.3% Triton X-100 that was applied for 2 hours at room temperature to block nonspecific binding. Primary antibodies against VDR (1:100, 12550; Cell Signaling Technology, Danvers, MA, USA) and Collagen I (1:400, ab88147; Abcam, Cambridge, MA, USA) were diluted in the dilution buffer (containing 3% normal donkey serum, 0.5% bovine serum albumin, and 0.3% Triton X-100 in 0.1 M PBS), which covered the sections during overnight incubation at 4°C. After washing the sections three times with PBS for 5 minutes each, they were incubated with secondary antibodies for 2 hours at room temperature with either donkey anti-rat IgG (H+L) conjugated to Alexa Fluor 488 (1:400, A-21208; Invitrogen) or donkey anti-rabbit IgG (H+L) conjugated to Alexa Fluor 555 (1:400, A-31572; Invitrogen). The secondary antibodies were diluted in the same solution as the primary antibody. Finally, cell nuclei were stained with 4′,6-diamidino-2-phenylindole (Vector Laboratories, Burlingame, CA, USA). The images were captured with a Zeiss LSM 880 confocal microscope (ZEISS, Göttingen, Germany) under a ×20 magnification objective.

Statistical Analysis

Statistical Package for the Social Sciences (SPSS version 16.0; Chicago, IL, USA) software was used for analyses. A paired sample *t*-test evaluated the differences in quantitative RT-PCR (qRT-PCR values) between FD-T and FD-F eyes in the same mouse. For comparisons of two groups, independent data sets were compared by unpaired two-tailed *t*-tests. Multiple comparisons were performed using one-way ANOVA test or two-way ANOVA with Bonferroni's post hoc tests. For time-dependent multiple comparisons, a two-way repeated-measures ANOVA was used to calculate the significance of differences in ocular refractive parameters and ocular biometrics between the FD-T and FD-F eyes. Unless stated otherwise, data are presented as mean ± SEM. P values < 0.05 were considered statistically significant.

Results

Form Deprivation Suppresses Scleral *Vdr* mRNA Expression Levels

The effects of 14 days of FD on scleral *Vdr* mRNA expression levels were determined in 3-week-old C57BL/6J male mice ($n = 12$). Form deprivation induced significant myopia in the FD (T-F) group compared with the NC (OD-OS) group (FD versus NC group: −5.87 ± 1.23D versus −0.12 ± 0.46D,

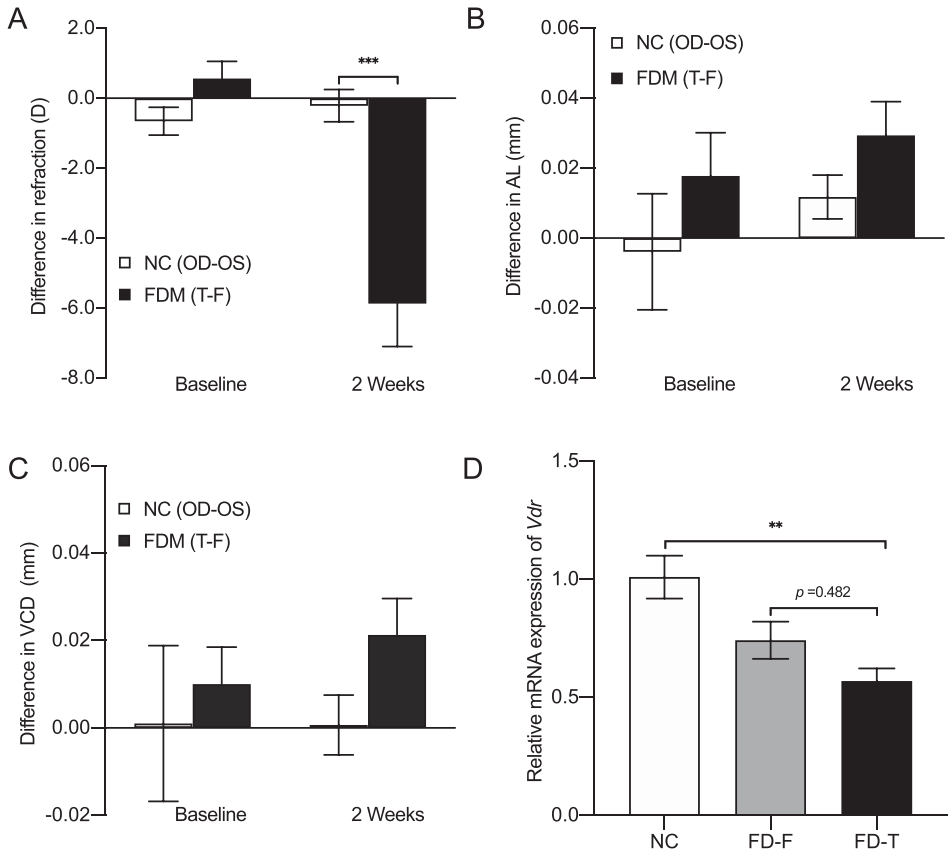

Figure 1. Form deprivation downregulates scleral *Vdr* mRNA expression levels. (**A**) The FD group after 2 weeks of monocular form deprivation was significantly more myopic than the age-matched NC. There are no significant changes in AL (**B**) and VCD (**C**) following 2 weeks of FD. The C57BL/6J mice were randomly assigned to different groups. FD (T-F) = differences between FD-T and FD-F eyes in the same mice ($n = 7$); NC (OD-OS) = differences between oculus dexter (OD) and oculus sinister (OS) eyes in the age-matched unoccluded mice ($n = 5$). (**D**) qRT-PCR analyses showed that scleral *Vdr* mRNA levels reduced significantly in the FD-T group at 2 weeks relative to that in the NC group ($n = 4$, $P = 0.0081$), whereas this difference was not significant between FD-F and FD-T eyes ($n = 4$, $P = 0.4282$). Relative quantification (RQ) values were normalized to an internal *18S rRNA* mouse control; repeated-measures ANOVA measured the refraction. RQ values were calculated using the one-way ANOVA test. *$P < 0.05$, **$P < 0.01$, ***$P < 0.001$, ****$P < 0.0001$. The data shown on the y-axes are expressed as mean ± SEM.

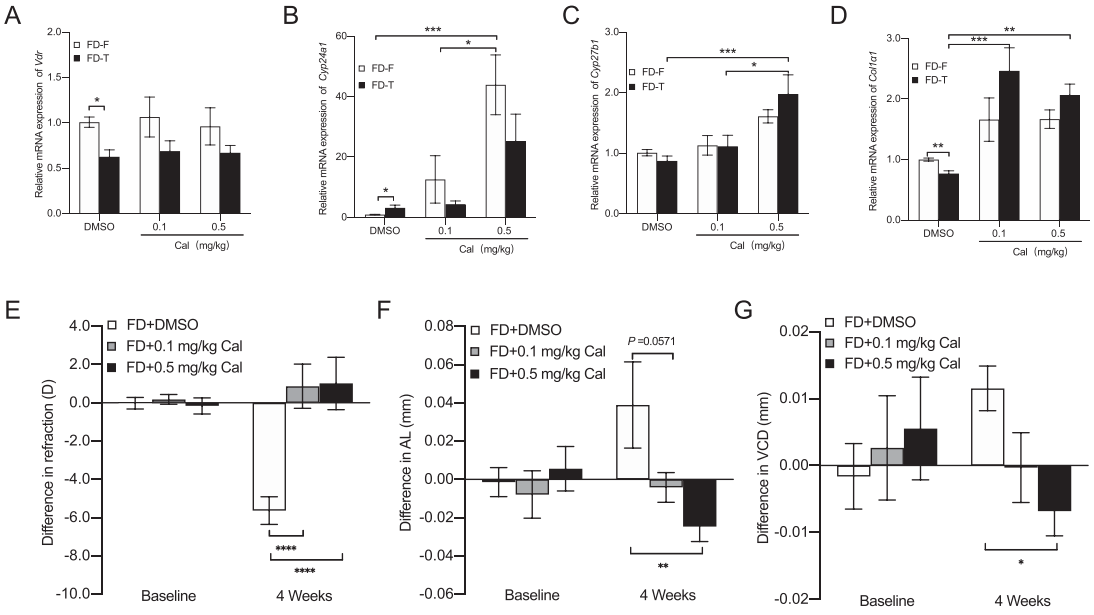

Figure 2. Calcipotriol blocks FD changes in refraction, AL, and VCD through upregulating *Col1α1* gene expression levels in a normal vision environment. (**A–D**) Levels of scleral *Vdr* (**A**), *Cyp24a1* (**B**), *Cyp27b1* (**C**), and *Col1α1* (**D**) mRNA were determined by qRT-PCR analysis after 4 weeks of FD and either DMSO or calcipotriol injections (DMSO n = 8, 0.1mg/kg Cal n = 7, 0.5mg/kg Cal n = 8). *Col1α1* (**D**) mRNA upregulation after 4 weeks of Cal injection in the FD group relative to the changes in the DMSO treated FD group. (**E–G**) Intraperitoneal calcipotriol injections reduced myopia progression in refraction (**E**), AL (**F**), and VCD (**G**). FD data expressed as mean difference between FD-T and FD-F at each time point (FD+DMSO n = 15, FD+0.1mg/kg Cal n = 15, FD+0.5mg/kg Cal n = 15). *18S rRNA* was used as a reference gene. Significance was determined between the gene expression values in the FD-T and the FD-F eyes with a paired sample *t*-test. Multiple comparisons were performed using a two-way ANOVA test. (**E–G**) Data were analyzed using repeated-measures ANOVA, $^{*}P < 0.05$, $^{**}P < 0.01$, $^{***}P < 0.001$, $^{****}P < 0.0001$.

$P = 0.0002$, Fig. 1A). On the other hand, there were no significant changes in the AL (FD versus NC group: 0.012 ± 0.006 mm versus 0.029 ± 0.01 mm, $P = 0.6212$, Fig. 1B) and VCD (FD versus NC group: 0.001 ± 0.007 mm versus 0.021 ± 0.008 mm, $P = 0.372$, Fig. 1C) between the FD (T-F) and NC (OD-OS) groups. After 2 weeks of FD, the *Vdr* mRNA levels were significantly lower in the FD-T eyes than in the NC eyes ($P = 0.0081$, Fig. 1D) whereas the difference was not significant between the FD-T and FD-F groups ($P = 0.4282$, Fig. 1D). Furthermore, Fig. 2A indicates that, after 4 weeks of FD, the *Vdr* mRNA levels were significantly lower in the FD-T eyes than in the FD-F eyes in the DMSO group ($P = 0.0103$). These changes suggest that *Vdr* gene expression progressively fell to reach levels that were significantly less than those in the FD-F eyes during the course of myopia progression.

Calcipotriol Inhibits FDM Progression Without Altering Normal Refractive Development

We then determined if activation of *Vdr* signaling could inhibit myopia development through suppressing the decline in the scleral *Col1α1* expression. To activate the scleral *Vdr* signaling, we performed intraperitoneal injections of either 0.1 mg/kg or 0.5mg/kg calcipotriol, and the mice injected with the DMSO-containing vehicle served as the control. In the first stage, we assessed the effect of calcipotriol injection on normal refractive development. After 4 weeks of injections, there were no significant differences in *Vdr*, *Cyp24a1*, *Cyp27b1*, and *Col1α1* mRNA expressions among the three groups (Supplementary Figs. S1A–D). Vitamin D3 is activated through hydroxylations by CYP27B1 and inactivated by CYP24A1.[33] Calcipotriol injections did not alter either the refraction, AL or VCD (Supplementary Figs. S1E–G) in non-FD mice. In the second stage, we determined the effects of intraperitoneal injections on FDM development. Four weeks of FD induced a significant decline in *Vdr* (Fig. 2A, $P = 0.0103$) and *Col1α1* (Fig. 2D, $P = 0.0019$) mRNA levels in FD-T eyes than those in FD-F eyes in the DMSO group. However, such declines were not observed on comparing the FD-F eyes of DMSO and calcipotriol groups (Figs. 2A, D, DMSO versus 0.5 mg/kg or 0.1 mg/kg Cal, $P > 0.9999$). Calcipotriol maintained the stability of scleral *Vdr* by sustaining *Cyp24a1* (Fig. 2B, $P = 0.0003$) and *Cyp27b1* (Fig. 2C, $P = 0.0007$) expression levels. These results suggest that calcipotriol only reduces the mRNA expression level of *Vdr* difference within groups, whereas its effects across groups were insignificant. After 4 weeks of FD, calcipotriol decreased the myopia development compared to the DMSO-injected group (Fig. 2E, 0.5 mg/kg Cal versus 0.1 mg/kg Cal versus DMSO: 1.01 ± 1.37 D versus 0.87 ± 1.16 D versus −5.63 ± 0.72 D; $n = 15$ in each group, $P < 0.0001$). This myopia inhibition was accompanied by suppressed AL elongations in the calcipotriol groups (Fig. 2F, 0.5 mg/kg Cal versus 0.1 mg/kg Cal versus DMSO: 0.039 ± 0.023 mm versus −0.004 ± 0.008 mm versus −0.025 ± 0.008 mm, DMSO versus 0.1 mg/kg Cal, $P = 0.0571$; DMSO versus 0.5 mg/kg Cal, $P = 0.0021$). In the FD group, the VCD was significantly less in the mice injected with 0.5 mg/kg calcipotriol (−0.007 ± 0.004 mm) compared to those injected with DMSO (0.012 ± 0.003 mm) (Fig. 2G, DMSO versus 0.1 mg/kg Cal, $P = 0.2504$; DMSO versus 0.5 mg/kg Cal, $P = 0.0478$). Therefore, calcipotriol inhibited the FDM-induced declines in *Vdr* and *Col1α1* mRNA expression within the group,

Investigative Ophthalmology & Visual Science

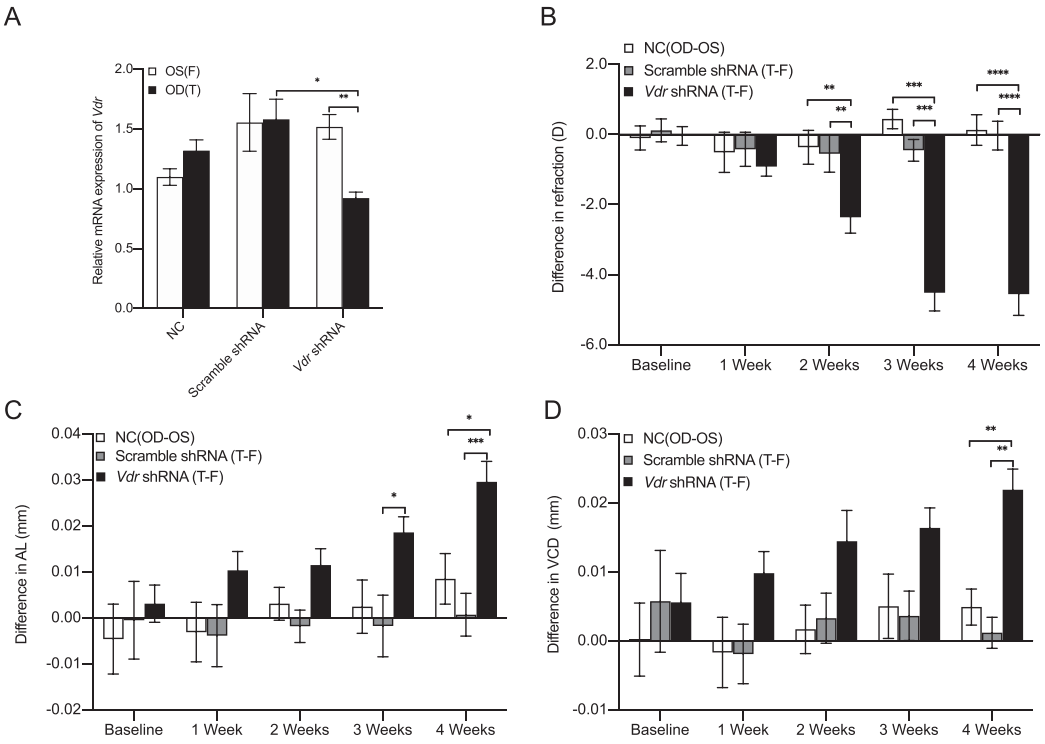

Figure 3. *Vdr* shRNA transfection reduces *Vdr* gene expression levels and increases refraction, AL, and VCD. (**A**) qRT-PCR analysis of *Vdr* mRNA expression in sclera. *Vdr* shRNA transfection reduced *Vdr* gene expression by 42%. The solid black bar represents the results of injection with either *Vdr* shRNA or scrambled shRNA; the unshaded open bar served as the fellow (F) control (n = 7). Data from age-matched mice with no treatment are also presented for comparison (NC, n = 6). Gene expression levels were normalized to *18S rRNA* control. (**B–D**) Four weeks after injection of *Vdr* shRNA, significant differences were observed in interocular differences in refraction, AL, and VCD between the scrambled shRNA and the NC groups at the indicated postnatal time points during normal refractive development. The unshaded bar of the NC (OD-OS) group shows the refraction, AL and VCD differences between the right and left eyes in the age-matched NC mice (n = 18). *Gray bar* of the scrambled shRNA (T-F) group shows the interocular differences between the injection-treated (T) eyes and noninjected fellow (F) eyes in sub-Tenon's capsule injected with an irrelevant scrambled sequence (n = 18). The *solid black bar* of the *Vdr* shRNA (T-F) group shows the interocular differences between the T and F eyes and those injected with mouse *Vdr* gene shRNA (n = 22). The effect of injection on time-dependent refractive development was evaluated by multivariate analysis of variance. RQ values were calculated using the one-way ANOVA test. Data were expressed as mean ± SEM. *$P < 0.05$, **$P < 0.01$, ***$P < 0.001$, ****$P < 0.0001$.

which accounts for why their expression levels were similar to those in the FD-F group.

Scleral *Vdr* Knockdown Induces Myopia Development

To determine if scleral VDR downregulation contributes to myopia development by reducing COL1α1 expression, we assessed the effect of scleral *Vdr* knockdown on normal refractive development. After 4 weeks of *Vdr* shRNA injection, the *Vdr* mRNA expression level of the injected eyes was lower than that in the noninjected fellow eyes (Fig. 3A, $P = 0.0314$) or the AAV8-Scramble injected eyes (Fig. 3A, $P = 0.023$).

Baseline measurements of all biometric variables were similar among the three groups and between the eyes of individual mice in the same group (Fig. 3B). After 2, 3, or 4 weeks of AAV8 injection, the refraction in *Vdr* shRNA-injected eyes was significantly more myopic than the AAV8-Scramble eyes and the NC groups (Fig. 3B, NC versus Scramble shRNA versus *Vdr* shRNA: 0.127 ± 0.437 diopters [D] versus −0.032 ± 0.409 D versus −4.559 ± 0.603 D, NC/Scramble shRNA versus *Vdr* shRNA, $P < 0.0001$). Consistent with the refraction, the AL elongation (Fig. 3C, NC versus Scramble shRNA versus *Vdr* shRNA: 0.008 ± 0.005 mm versus 0.001 ± 0.005 mm versus 0.03 ± 0.004 mm, NC versus *Vdr* shRNA, $P = 0.0108$; Scramble shRNA versus *Vdr* shRNA, $P = 0.0002$) and VCD increase (Fig. 3D, NC versus Scramble shRNA versus *Vdr* shRNA: 0.0049 ± 0.003 mm versus 0.001 ± 0.002 mm versus 0.022 ± 0.003 mm, NC versus *Vdr* shRNA, $P = 0.01$; Scramble shRNA versus *Vdr* shRNA, $P = 0.0011$) were observed in AAV8-shRNA–injected eyes. Details of the values and comparisons of interocular differences are provided in Supplementary Tables S1 and S2. Taken together, scleral *Vdr* downregulation induced a significant myopic shift in refraction as well as increases in the AL and VCD.

Calcipotriol Upregulates COL1A1 Expression Through a VDR-Dependent Signaling Pathway in HSFs

To evaluate the importance of VDR-dependent signaling pathway in controlling COL1A1 expression, we treated the HSFs with different concentrations of calcipotriol. As per the minimum information for publication of quantitative real-time PCR experiments (MIQE) guidelines,[35] we have

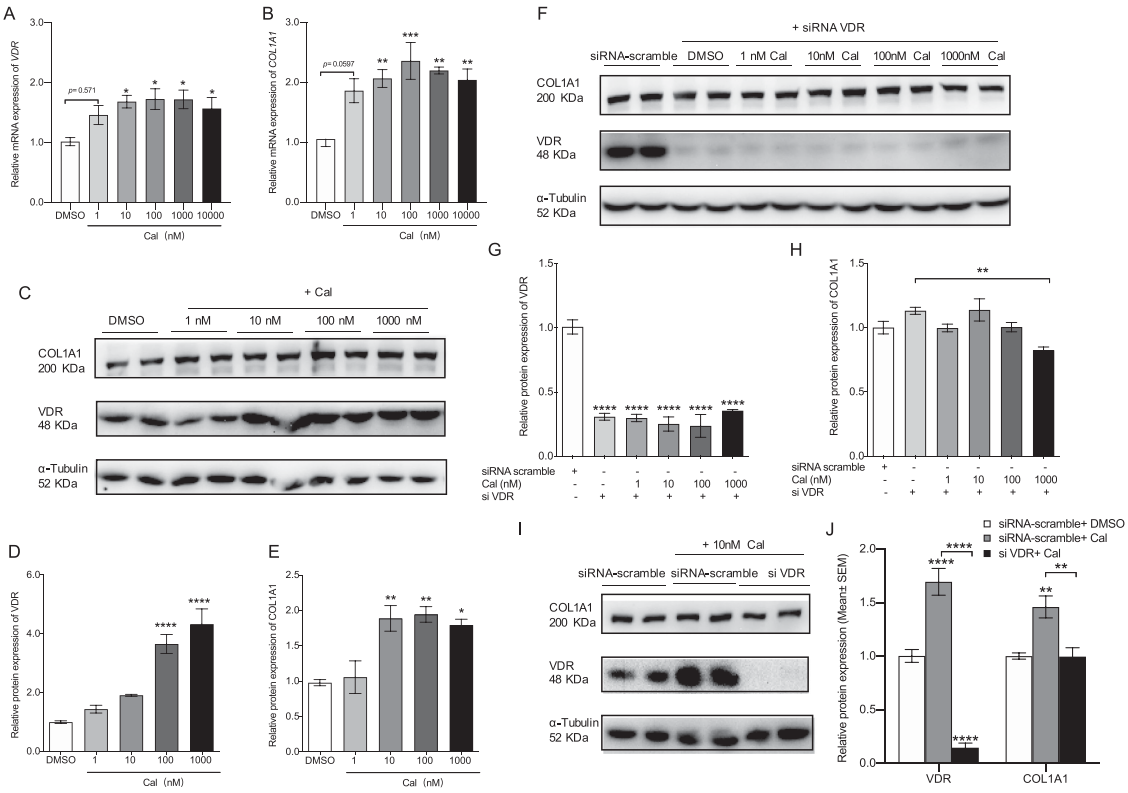

Figure 4. Calcipotriol upregulates COL1A1 protein expression levels through a VDR-dependent pathway in HSFs. Dose-dependent (1 nM, 10 nM, 100 nM, 1 µM, 10 µM) effects of calcipotriol on *VDR* and *COL1A1* mRNA levels are shown in panels **A** and **B**. (**C–E**) Corresponding effects of calcipotriol are shown on VDR and COL1A1 protein expression levels. (**F–H**) Western blot analysis evaluated the effects of the loss of VDR function on calcipotriol-induced increases in COL1A1 protein expression. (**I**, **J**) Western blot analysis evaluated the effects of the loss of VDR function on 10-nM calcipotriol-induced increases in COL1A1 protein expression. *ACTB* (Supplementary Fig. S3A) was used as an internal control in mRNA levels (**A**, **B**). α-Tubulin as a loading equivalence control on the Western blots (**C**), the bar (**D**, **E**) graphs represent relative protein expression levels of VDR and COL1A1 from grayscale analysis using Photoshop. Similarly, Figures 4G and 4H are summary plots of the results shown in Figure 4F. Figure 4J shows summary plots of the results shown in Figure 4I. Results are expressed as mean ± SEM of four independent analyses in Western blots and eight independent analyses in qRT-PCR. $^{*}P < 0.05$, $^{**}P < 0.01$, $^{***}P < 0.001$, $^{****}P < 0.0001$. (**A–E**) Multiple comparisons were performed by using one-way analysis of variance with Bonferroni's post hoc test and (**F–J**) ordinary two-way ANOVA.

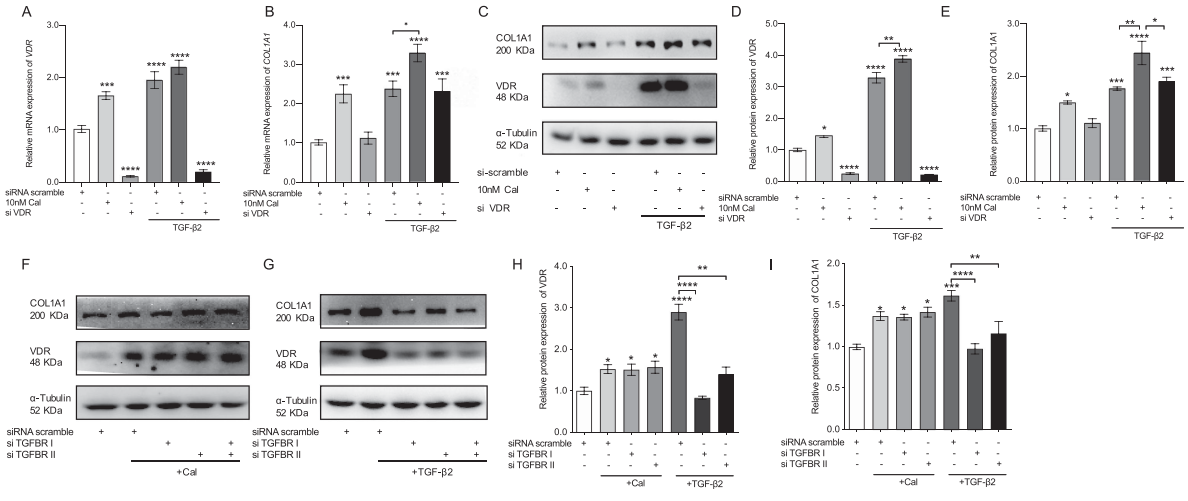

Figure 5. TGF-β2 induces increases in collagen expression levels through a VDR-independent signaling pathway. (**A–E**) Activation and inhibition of VDR expression-induced changes in COL1A1 protein expression are compared in the presence and absence of TGF-β2 (5 ng/mL) for 24 hours in HSFs. *VDR* (**A**) and *COL1A1* (**B**) mRNA expression levels were determined by qRT-PCR with *ACTB* (Supplementary Fig. S3B) as an internal control with eight independent analyses. Western blot analysis evaluated VDR (**D**) and COL1A1 (**E**) protein expression with α-tubulin as an internal control on the same blots. (**F–I**) HSFs were transfected with a relevant *TGFBRI* or *TGFBRII* siRNA and were then exposed to calcipotriol (10 nM) or TGF-β2 (5 ng/mL) for 24 hours. Western blot analysis of VDR and COL1A1 protein expression levels of each treatment group, VDR (**H**), and COL1A1 (**I**) protein expression data are expressed as mean ± SEM in triplicate by scanning volumetric densitometry. α-Tubulin was used to verify protein loading equivalence. $^{*}P < 0.05$, $^{**}P < 0.01$, $^{***}P < 0.001$, $^{****}P < 0.0001$; two-way ANOVA test.

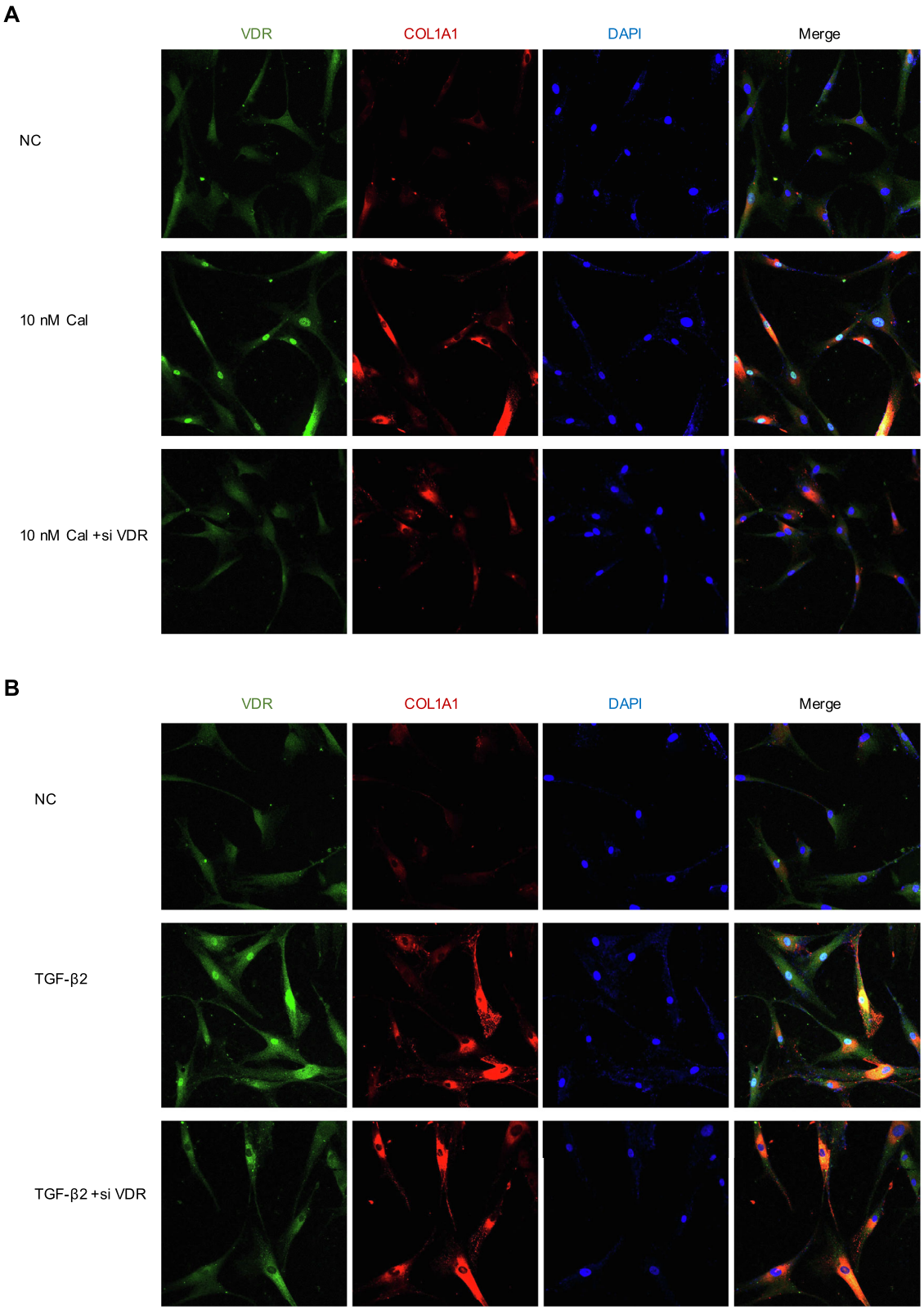

Figure 6. Calcipotriol and TGF-β2 induce increases in COL1A1 expression through parallel signaling pathways. (**A–D**) Images depict COL1A1 protein (*red*) and VDR protein (*green*) immunoreactivity and the blue delimited 4′,6-diamidino-2-phenylindole nuclear staining. (**A**) Calcipotriol upregulates COL1A1 expression through a VDR-dependent pathway. (**B**) TGF-β2–induced increases in COL1A1 protein expression level were not blocked by VDR siRNA-transfected HSFs. (**C**) Interference with both *TGFBRI* and *TGFBRII* did not mask the expression of VDR and COL1A1 induced by 10 nM calcipotriol, (**D**) while interference with both TGFBRI and TGFBRII may have masked the expression of VDR and collagen induced by TGF-β2. *Scale bar*: 50 µm.

Investigative Ophthalmology & Visual Science

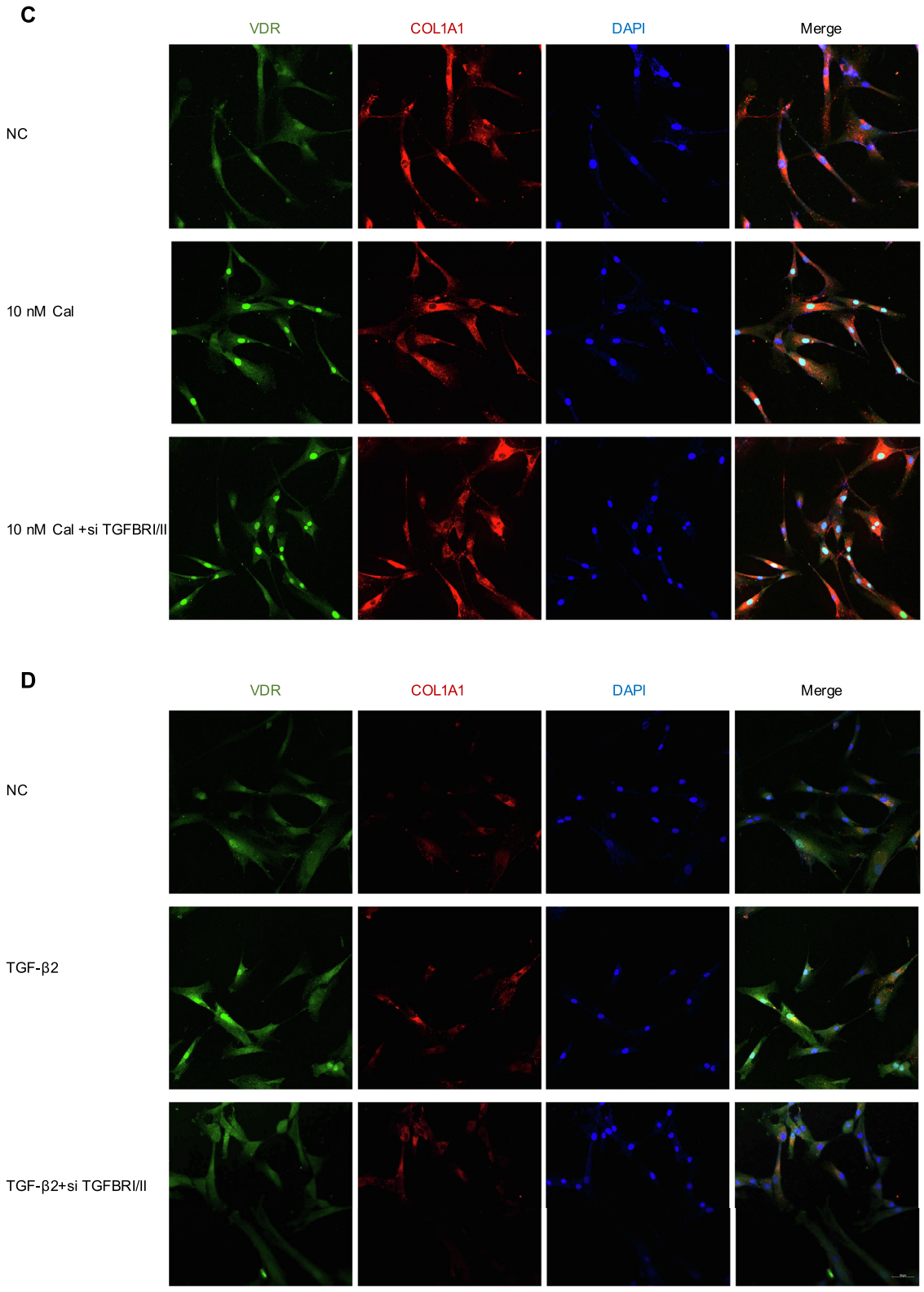

Figure 6. Continued.

normalized the expression of *VDR* and *COL1A1* and applied them across different treatment paradigms using multiple reference genes such as *ACTB*, *GAPDH*, and *HPRT* (Supplementary Figs. S2A and S2B). There is no significant difference in the expression levels of these target genes irrespective of the reference gene used. Hence, we used one reference gene in subsequent qRT-PCR experiments. After 24 hours of treatment, calcipotriol dose dependently increased both *VDR* and *COL1A1* mRNA expression up to levels in the 100-nM group (Figs. 4A, 4B, DMSO versus 100

Investigative Ophthalmology & Visual Science

nM Cal, $P = 0.0207$, $P = 0.0002$). These upregulations were accompanied by corresponding increases in the protein expression levels of VDR and COL1A1 (Figs. 4D, 4E, DMSO versus 100 nM Cal, $P < 0.0001$, $P = 0.0031$). In addition, loss of VDR function by siRNA transfection obviated the calcipotriol-induced rises in VDR protein expression levels (Fig. 4G, $P < 0.0001$). Loss of VDR function blocked the increases in COL1A1 protein expression levels at all exogenous calcipotriol concentrations (Fig. 4H). Accordingly, 10 nM was used to evaluate the involvement of VDR signaling in mediating increases in COL1A1 expression in HSFs under the subsequent conditions. Loss of *VDR* gene function blocked the respective increases in VDR and COL1A1 protein expression levels induced by 10 nM calcipotriol (Fig. 4J, $P < 0.0001$, $P = 0.0013$). Taken together, calcipotriol-induced rises in COL1A1 protein expression levels depend on *VDR* gene function in HSFs.

TGF-β2 Induces Increases in COL1A1 Expression Through a VDR-Independent Signaling Pathway

TGF-β2 is involved in mediating scleral ECM changes and myopia progression in animal models.[26,36] We determined whether calcipotriol induced increases in COL1A1 through a TGF-β2–dependent way in HSFs. The individual effects of TGF-β2 (5 ng/mL) and calcipotriol (10 nM) on COL1A1 expression were measured in HSFs transfected with either *VDR* siRNA or *TGFBRI/II* siRNA. TGF-β2 treatment alone increased both *VDR* and *COL1A1* mRNA and protein expression levels (Fig. 5). While both TGF-β2 and calcipotriol upregulated *VDR* gene expression, they were suppressed in *VDR* siRNA-transfected HSFs. (Figs. 5A, 5D, lane 1 versus lane 3/6, $P < 0.0001$). However, the loss of VDR function in siRNA-transfected cells did not reduce the TGF-β2–induced increase in COL1A1 protein expression (Figs. 5B, 5E, lane 4 versus lane 6, $P > 0.9999$), which suggests that there is another VDR-independent signaling pathway through which TGF-β upregulates COL1A1. Another indication of the existence of such a pathway is that combining calcipotriol and TGF-β2 increased the *COL1A1* gene and protein expression to levels that exceeded those obtained with TGF-β2 alone (Figs. 5B, 5E, lane 4 versus lane 5, $P = 0.0018$, $P = 0.0013$). To evaluate whether calcipotriol and TGF-β2 mediate control of COL1A1 expression levels through parallel noninteracting receptor-linked signaling pathways, the individual effects of 10 nM calcipotriol and 5 ng/mL TGF-β2 were compared with one another in *TGFBRI/II* siRNA-transfected HSFs and in scrambled siRNA-transfected HSFs. Calcipotriol induced increases in VDR and COL1A1 protein expression levels that were not blocked in *TGFBRI* or *TGFBRII* siRNA-transfected HSFs (Figs. 5F, 5H, 5I, lane 2 versus lane 3/4, $P > 0.9999$). However, TGF-β2–induced increases in the expression of VDR and COL1A1 were essentially mediated through TGFBRI/II (Figs. 5H, 5I, lane 5 versus lane 6, $P < 0.0001$). Immunostaining signals were also consistent with these results (Fig. 6). These data suggest that calcipotriol and TGF-β2 induced increases in COL1A1 expression levels through two different signaling pathways.

Discussion

There is growing evidence showing that vitamin D is endogenously produced by ocular tissues.[37–39] VDR expression is evident in the epithelium of the cornea,[40] lens, ciliary body, and retinal pigment epithelium as well as the corneal endothelium, retinal ganglion cell layer, and photoreceptors.[40,41] Given that VDR and vitamin D hydroxylases (CYP24A1 and CYP27B1) are expressed throughout the eye, characterizing their roles is a relevant approach to uncovering mechanisms that control ocular function in health and disease.

Our results suggest that upregulating scleral VDR expression levels may be a viable option to suppress myopia development in a clinical setting. This is evident since scleral *Vdr* expression was downregulated during myopia development in a well-recognized FDM mouse model. Scleral *Vdr* downregulation also induced declines in *Col1α1* expression and myopia development. Finally, calcipotriol injections reversed the FD-induced declines in the *Col1α1* expression level and markedly inhibited myopia progression. At the same time, calcipotriol maintained the scleral *Vdr* levels by regulating the expressions of *Cyp24a1* and *Cyp27b1*. However, calcipotriol injections had no effect on ocular development in a normal refractive development.

TGF-β exists in three different isoforms (β1, β2, β3) that increase both COL1A1 expression levels and stimulate fibroblast proliferation in the mammalian sclera.[25,26] TGF-β2 levels are significantly reduced during myopia development.[25,42] Such declines may contribute to long-term collagen fibril diameter thinning observed in highly myopic eyes.[43,44] A complex interplay between the TGF-β and VDR signaling pathways has been described in recent studies in different tissues,[28–30,45,46] and they define a role for VDR as an endocrine checkpoint to modulate liver fibrosis.[28] On the other hand, vitamin D3 increased the expression of TGF-β and TGFBRI/II in osteoblasts[47] and patients with multiple sclerosis.[48] Therefore, the interplay between TGF-β and vitamin D3 can be either synergistic or antagonistic. Our results show that calcipotriol and TGF-β2 induce increases in COL1A1 mRNA and protein expression levels through parallel independent signaling pathways in HSFs. On the other hand, the VDR and TGF-β2 signaling pathways are likely to interact with one another, as TGF-β2 upregulated VDR protein expression, without having a corresponding effect on COL1A1 expression level. Therefore, the interaction between vitamin D3 and TGF-β in mediating control of COL1A1 is tissue specific. The role of vitamin D3 is unclear and perhaps species specific, as it was earlier shown that it had no impact on myopia development in tree shrews (Siegwart JT, et al. *IOVS* 2011;52(14):ARVO E-Abstract 6298). Future studies are still required to determine if the protective effects of vitamin D3 against myopia in our study can be replicated in a clinical setting.

It must be noted that the prevalence of low vitamin D is common across different parts of the world.[49] However, a direct relation between regions with low vitamin D levels and increased prevalence of myopia could not be established. This could be due to a variety of environmental variables, including the level of education,[50] time spent on near work,[51] profession,[52] and so on, all of which are confounding factors for myopia development. Due to the complex interactions of genetic and environmental factors in myopia, vitamin D3 may regulate the expression of COL1A1 in more than one way to inhibit the progression of myopia. It was earlier reported that vitamin D increased the activity of matrix degrading enzymes, MMP-9 and MMP-2, and suppressed the levels of their moderator, TIMP-1, leading to reduced ECM and collagen deposition in liver.[53] On the other hand, vitamin D treatment decreased activities of MMP-9[54] and TGF-β

Investigative Ophthalmology & Visual Science

levels and decreased collagen deposition in articular cartilage and lung fibrosis.[55] Given that the scleral ECM undergoes significant remodeling during myopia, we speculate that downregulation of VDR may contribute to this scleral remodeling that potentially leads to myopia development. Especially, studies focusing on vitamin D deficiency treatments and myopia progression in humans and other mammals could shed more light on vitamin D mechanisms in relation to myopia.

Acknowledgments

The authors thank Frank Schaeffel (Institute for Ophthalmic Research, Section of Neurobiology of the Eye, University of Tuebingen, Tuebingen, Germany) for providing support for our eccentric infrared photoretinoscope.

Supported by the National Natural Science Foundation of China grants 82025009 (to XZ), 81670886 (to XZ), 82171097 (to FZ), 81830027 (to JQ), U20A20364 (to JQ), and 81700868 (to FZ); Natural Science Foundation of Zhejiang Province (Zhejiang Provincial Natural Science Foundation) grant LQ16H120006 (to FZ); and Scientific Bureau of Wenzhou City grant H2020007 (to FZ) and Y20180731 (to SJ).

Disclosure: **S. Jiao**, None; **P.S. Reinach**, None; **C. Huang**, None; **L. Yu**, None; **H. Zhuang**, None; **H. Ran**, None; **F. Zhao**, None; **N. Srinivasalu**, None; **J. Qu**, None; **X. Zhou**, None

References

1. Alvarez-Peregrina C, Villa-Collar C, Martinez-Perez C, et al. Social media impact of myopia research. *Int J Environ Res Public Health*. 2022;19(12):7270.
2. Shan M, Dong Y, Chen J, et al. Global tendency and frontiers of research on myopia from 1900 to 2020: a bibliometrics analysis. *Front Public Health*. 2022;10:846601.
3. Spillmann L. Stopping the rise of myopia in Asia. *Graefes Arch Clin Exp Ophthalmol*. 2020;258(5):943–959.
4. Dolgin E. The myopia boom. *Nature*. 2015;519(7543):276–278.
5. Lin MY, Lin IT, Wu YC, et al. Stepwise candidate drug screening for myopia control by using zebrafish, mouse, and Golden Syrian Hamster myopia models. *EBioMedicine*. 2021;65:103263.
6. Harper AR, Summers JA. The dynamic sclera: extracellular matrix remodeling in normal ocular growth and myopia development. *Exp Eye Res*. 2015;133:100–111.
7. Verhoeven VJ, Hysi PG, Wojciechowski R. Genome-wide meta-analyses of multiancestry cohorts identify multiple new susceptibility loci for refractive error and myopia. *Nat Genet*. 2013;45(3):314–318.
8. Enthoven CA, Tideman JWL, Polling JR, et al. Interaction between lifestyle and genetic susceptibility in myopia: the Generation R study. *Eur J Epidemiol*. 2019;34(8):777–784.
9. Tideman JWL, Polling JR, Jaddoe VWV, et al. Environmental risk factors can reduce axial length elongation and myopia incidence in 6- to 9-year-old children. *Ophthalmology*. 2019;126(1):127–136.
10. Li YJ, Guggenheim JA, Bulusu A, et al. An international collaborative family-based whole-genome linkage scan for high-grade myopia. *Invest Ophthalmol Vis Sci*. 2009;50(7):3116–3127.
11. Lingham G, Mackey DA, Zhu K, et al. Time spent outdoors through childhood and adolescence—assessed by 25-hydroxyvitamin D concentration—and risk of myopia at 20 years. *Acta Ophthalmol*. 2021;99(6):679–687.
12. Jung BJ, Jee D. Association between serum 25-hydroxyvitamin D levels and myopia in general Korean adults. *Indian J Ophthalmol*. 2020;68(1):15–22.
13. Choi JA, Han K, Park YM, et al. Low serum 25-hydroxyvitamin D is associated with myopia in Korean adolescents. *Invest Ophthalmol Vis Sci*. 2014;55(4):2041–2047.
14. Tideman JW, Polling JR, Voortman T, et al. Low serum vitamin D is associated with axial length and risk of myopia in young children. *Eur J Epidemiol*. 2016;31:491–499.
15. Tang SM, Tiffany L, Rong SS, et al. Vitamin D and its pathway genes in myopia: systematic review and meta-analysis. *Br J Ophthalmol*. 2019;103(1):8–17.
16. Mutti DO, Cooper ME, Dragan E, et al. Vitamin D receptor (VDR) and group-specific component (GC, vitamin D-binding protein) polymorphisms in myopia. *Invest Ophthalmol Vis Sci*. 2011;52(6):3818–3824.
17. Harb EN, Wildsoet CF. Nutritional factors and myopia: an analysis of national health and nutrition examination survey data. *Optom Vis Sci*. 2021;98(5):458–468.
18. Li X, Lin H, Jiang L, et al. Low serum vitamin D is not correlated with myopia in Chinese children and adolescents. *Front Med (Lausanne)*. 2022;9:809787.
19. Cuellar-Partida G, Williams KM, Yazar S, et al. Genetically low vitamin D concentrations and myopic refractive error: a Mendelian randomization study. *Int J Epidemiol*. 2017;46(6):1882–1890.
20. Reichrath J, Muller SM, Kerber A, et al. Biologic effects of topical calcipotriol (MC 903) treatment in psoriatic skin. *J Am Acad Dermatol*. 1997;36:19–28.
21. Bury Y, Ruf D, Hansen CM, et al. Molecular evaluation of vitamin D3 receptor agonists designed for topical treatment of skin diseases. *J Invest Dermatol*. 2001;116(5):785–792.
22. Peng Y, Wu M, Alvarez JA, et al. Vitamin D status and risk of cystic fibrosis-related diabetes: a retrospective single center cohort study. *Nutrients*. 2021;13(11):4048.
23. Gao N, Li X, Kong M, et al. Associations between vitamin D levels and risk of heart failure: a bidirectional Mendelian randomization study. *Front Nutr*. 2022;9:910949.
24. Wang YQ, Geng XP, Wang MW, et al. Vitamin D deficiency exacerbates hepatic oxidative stress and inflammation during acetaminophen-induced acute liver injury in mice. *Int Immunopharmacol*. 2021;97:107716.
25. McBrien NA. Regulation of scleral metabolism in myopia and the role of transforming growth factor-beta. *Exp Eye Res*. 2013;114:128–140.
26. Jobling AI, Nguyen M, Gentle A, et al. Isoform-specific changes in scleral transforming growth factor-beta expression and the regulation of collagen synthesis during myopia progression. *J Biol Chem*. 2004;279(18):18121–18127.
27. Li X, Yong T, Wei Z, et al. Reversing insufficient photothermal therapy-induced tumor relapse and metastasis by regulating cancer-associated fibroblasts. *Nat Commun*. 2022;13(1):2794.
28. Ding N, Yu RT, Subramaniam N, et al. A vitamin D receptor/SMAD genomic circuit gates hepatic fibrotic response. *Cell*. 2013;153(3):601–613.
29. Zerr P, Vollath S, Palumbo-Zerr K, et al. Vitamin D receptor regulates TGF-β signalling in systemic sclerosis. *Ann Rheum Dis*. 2015;74(3):20.
30. Kitami K, Yoshihara M, Tamauchi S, et al. Peritoneal restoration by repurposing vitamin D inhibits ovarian cancer dissemination via blockade of the TGF-β1/thrombospondin-1 axis. *Matrix Biol*. 2022;109:70–90.
31. Pan M, Zhao F, Xie B, et al. Dietary ω-3 polyunsaturated fatty acids are protective for myopia. *Proc Natl Acad Sci USA*. 2021;118(43):2104689118.

32. Qu J, Zhou X, Xie R, et al. The presence of m1 to m5 receptors in human sclera: evidence of the sclera as a potential site of action for muscarinic receptor antagonists. *Curr Eye Res*. 2006;31(7–8):587–597.
33. Markiewicz A, Brożyna AA, Podgórska E, et al. Vitamin D receptors (VDR), hydroxylases CYP27B1 and CYP24A1 and retinoid-related orphan receptors (ROR) level in human uveal tract and ocular melanoma with different melanization levels. *Sci Rep*. 2019;9:9142–9155.
34. Schmittgen TD, Livak KJ. Analyzing real-time PCR data by the comparative C(T) method. *Nat Protoc*. 2008;3(6):1101–1108.
35. Bustin SA, Benes V, Garson JA, et al. The MIQE guidelines: minimum information for publication of quantitative real-time PCR experiments. *Clin Chem*. 2009;55(4):611–622.
36. Jobling AI, Gentle A, Metlapally R, et al. Regulation of scleral cell contraction by transforming growth factor-beta and stress: competing roles in myopic eye growth. *J Biol Chem*. 2009;284(4):2072–2079.
37. Rullo J, Pennimpede T, Mehraban Far P, et al. Intraocular calcidiol: uncovering a role for vitamin D in the eye. *J Steroid Biochem Mol Biol*. 2020;197:105536.
38. Alsalem JA, Patel D, Susarla R, et al. Characterization of vitamin D production by human ocular barrier cells. *Investig Ophthalmol Vis Sci*. 2014;55:2140–2147.
39. Chan HN, Zhang XJ, Ling XT, et al. Vitamin D and ocular diseases: a systematic review. *Int J Mol Sci*. 2022;23(8):4226.
40. Yin Z, Pintea V, Lin Y, et al. Vitamin D enhances corneal epithelial barrier function. *Invest Ophthalmol Vis Sci*. 2011;52(10):7359–7364.
41. Murugeswari P, Firoz A, Murali S, Vinekar A, et al. Vitamin-D3 (α-1, 25(OH) 2D3) protects retinal pigment epithelium from hyperoxic insults. *Invest Ophthalmol Vis Sci*. 2020;61(2):4.
42. Li T, Zhou X, Li B, et al. Effect of MT3 on retinal and choroidal TGF-beta2 and HAS2 expressions in form deprivation myopia of guinea pig. *J Ophthalmol*. 2017;2017:5028019.
43. Phillips JR, Khalaj M, McBrien NA. Induced myopia associated with increased scleral creep in chick and tree shrew eyes. *Invest Ophthalmol Vis Sci*. 2000;41(8):2028–2034.
44. Ouyang X, Han Y, Xie Y, et al. The collagen metabolism affects the scleral mechanical properties in the different processes of scleral remodeling. *Biomed Pharmacother*. 2019;118:109294.
45. Shirakata Y, Ueno H, Hanakawa Y, et al. TGF-beta is not involved in early phase growth inhibition of keratinocytes by 1alpha,25(OH)2vitamin D3. *J Dermatol Sci*. 2004;36(1):41–50.
46. Zhang Y, Mu Y, Ding H, et al. 1α,25-Dihydroxyvitamin D3 promotes angiogenesis after cerebral ischemia injury in rats by upregulating the TGF-β/Smad2/3 signaling pathway. *Front Cardiovasc Med*. 2022;9:769717.
47. Wu Y, Haugen JD, Zinsmeister AR, et al. 1 alpha,25-Dihydroxyvitamin D3 increases transforming growth factor and transforming growth factor receptor type I and II synthesis in human bone cells. *Biochem Biophys Res Commun*. 1997;239(3):734–739.
48. Shirvani-Farsani Z, Behmanesh M, Mohammadi SM, et al. Vitamin D levels in multiple sclerosis patients: association with TGF-beta2, TGF-betaRI, and TGF-betaRII expression. *Life Sci*. 2015;134:63–67.
49. Trollfors B. Ethnicity, gender and seasonal variations all play a role in vitamin D deficiency. *Acta Paediatr*. 2022;111(8):1596–1602.
50. Mountjoy E, Davies NM, Plotnikov D, et al. Education and myopia: assessing the direction of causality by mendelian randomisation. *BMJ*. 2018;361:2022.
51. Pärssinen O, Kauppinen M. Associations of near work time, watching TV, outdoors time, and parents' myopia with myopia among school children based on 38-year-old historical data. *Acta Ophthalmol*. 2022;100(2):430–438.
52. Schaeffel F. Myopia—what is old and what is new? *Optom Vis Sci*. 2016;93(9):1022–1030.
53. Abramovitch S, Dahan-Bachar L, Sharvit E, et al. Vitamin D inhibits proliferation and profibrotic marker expression in hepatic stellate cells and decreases thioacetamide-induced liver fibrosis in rats. *Gut*. 2011;60(12):1728–1737.
54. Li S, Niu G, Dong XN, et al. Vitamin D inhibits activities of metalloproteinase-9/-13 in articular cartilage in vivo and in vitro. *J Nutr Sci Vitaminol (Tokyo)*. 2019;65(2):107–112.
55. Schapochnik A, da Silva MR, Leal MP, et al. Vitamin D treatment abrogates the inflammatory response in paraquat-induced lung fibrosis. *Toxicol Appl Pharmacol*. 2018;355:60–67.

Investigative Ophthalmology & Visual Science